Journal of Cultural Heritage 29 (2018) 19–29

Available online at
ScienceDirect
www.sciencedirect.com

Elsevier Masson France
EM|consulte
www.em-consulte.com/en

Original article

X-ray fluorescence investigation on yellow pigments based on lead, tin and antimony through the comparison between laboratory and portable instruments

Giuseppe Capobianco [a], Claudia Pelosi [b,*], Giorgia Agresti [b], Giuseppe Bonifazi [a], Ulderico Santamaria [b], Silvia Serranti [a]

[a] Department of Chemical Engineering Materials and Environment, Sapienza-Rome university, Rome, Italy
[b] Laboratory of Diagnostics and Materials Science, University of Tuscia, Largo dell'Università, 01100 Viterbo, Italy

ARTICLE INFO

Article history:
Received 29 April 2017
Accepted 1st September 2017
Available online 28 September 2017

Keywords:
X-ray fluorescence spectroscopy
Lead-tin-antimony yellows
Principal component analysis
Multivariate analysis

ABSTRACT

This paper presents an investigation of yellow pigments based on lead, tin and antimony through X-ray fluorescence spectroscopy with the aim of comparing portable and laboratory instruments and discussing the potential application on artworks. Artificial yellow pigments, based on Pb-Sb-Sn, and produced in our laboratory, were chosen in order to have a well-known and already characterized sample set. The differentiation in artworks of these pigments is still a challenge if non-invasive portable X-ray spectrometers are used, as commonly occurs in practice. The analysis was performed by using the Bruker M4 Tornado laboratory equipment and the Assing Surface Monitor II portable apparatus. Scanning electron microscopy with energy dispersive spectroscopy was also applied for a semi-quantitative analysis of the chosen pigments. In order to perform a significant statistical comparison of acquired and processed data, all the analyses have been carried out by using the same sample, the same acquisition set-up and, at the same time, operative conditions for both instruments. A chemometric approach, based on the principal component analysis and multivariate analytical tools, was applied in order to verify the spectral differences, and related informative content, between the different produced yellow pigments. The multivariate approach revealed instrumental differences between the two systems and allowed the comparison of the common characteristics of the analyzed pigments set. The potential of this new approach is also linked to the possibility of differentiating artificial yellow pigments, both in terms of composition and, above all, in terms of recipes for their production.

1. Introduction

X-ray fluorescence (XRF) is a diagnostic approach particularly suited to use in cultural heritage since it falls under the class of non-destructive and non-invasive analytical tools [1–8]. Indeed, among the variety of non-invasive in situ techniques, XRF spectroscopy is one of the most widely utilized techniques in cultural heritage applications despite some intrinsic limitations [3–9]. Moreover, 2D scanning is possible with more recently developed instruments allowing the element distribution in a selected area of interest to be obtained [10–13].

Portable X-ray fluorescence (p-XRF) instruments and their applications have gained considerable attention within the archaeological community in recent years [14], but the skepticism regarding performance dominates debate today [15]. On the other hand, laboratory XRF based techniques have been a staple of archaeological science since the 1960s [16–19]. An appreciable number of these instruments in the past used radioactive isotopes rather than miniaturized X-ray tubes, making them difficult to transport across borders. So the term "portable" in XRF instruments has varied definitions, ranging from "being able to be carried by porters" [20] to "handheld" [21]. Portable XRF analyzers have approximately the size, shape, and weight of cordless drills and have a similar trigger. Weight and power consumption are also concerns for field use, however, the device sacrifices performance to gain portability [14]. The determination of the relationship between the intensity of the characteristic X-ray emission of an element and its concentration within a material is not simple and today it is possible only with benchtop XRF devices. In general, various effects, including the excitation of lighter elements by X-rays emitted from heavier elements and matrix effects, occur within a material, changing the measured intensities. Calibration standards

* Corresponding author. Tel.: +39 076 135 7673; Mobile +39 333 287 7468.
E-mail address: pelosi@unitus.it (C. Pelosi).

https://doi.org/10.1016/j.culher.2017.09.002
1296-2074/

("matrix matched") can be used to correct X-ray measurements. This analytical approach permits the quantification of the element in the analyzed matrix but it necessitates a priori knowledge of the "unknown material's" approximate composition. Therefore, the analyst's knowledge and experience are critical, in part, to recognize when data may be compromised by inappropriate calibrations [14–22]. The p-XRF measurement can be considered only for qualitative investigation, but recently, the analytical power of portable instruments has increased dramatically, and they are now frequently applied in mining, soil exploration and in the analysis of consumer goods [23]. The evolution of XRF devices has enabled the comparison of benchtop and portable instruments in different fields of research [24–26]. Modern benchtop XRFs are equipped with polycapillary optics that allow for generating high fluorescence intensities on even very small sample areas. The X-ray optics can focus tube radiation from a large solid angle to spots of less than 30 μm. Moreover, the vacuum chamber permits better detection of light elements [27]. In order to compare benchtop and portable XRF spectrometers efficiently, a multivariate approach is necessary, as widely discussed in the literature [3,12,28–31]. This approach makes possible the extraction of information on variance and dispersion of many acquisitions and it enables the spectral results from techniques based on the same physical principles to be understood [32–35]. In addition, a comparison of the signals obtained by portable and benchtop X-ray spectrometers allows the best set-up for p-XRF to be chosen in order to obtain signal quality similar to that of benchtop apparatus.

Using this general overview as a starting point, in the present paper, we chose to investigate the application of portable X-ray fluorescence (p-XRF) and benchtop XRF instruments in order to differentiate lead-tin-antimony based yellow pigments, whose preparation and composition is well-known, with the aim of making a comparison in terms of quality and reliability of the results on the same analytical sample set. To reach this goal, a comparison was carried out between portable and benchtop X-ray fluorescence devices applied on different types of yellow pigments based on lead, tin and antimony produced in our laboratory and characterized by different analytical techniques [36]. The yellow investigated were prepared according to the stoichiometry ratio of the chemical elements in the final compounds and according to the instructions described in "old" recipes [36–40]. Scanning electron microscopy (SEM) was also applied to the powder samples for a semi-quantitative analysis. The data obtained by XRF acquisitions were elaborated by principal component analysis (PCA) and multivariate analytical techniques in order to verify the spectral differences and the related informative content among the different yellow pigments produced [12,41–43]. Principal component analysis was chosen as a preliminary and explorative technique, which is particularly useful for comparing the results, obtained with the two spectrometers (benchtop and portable) tested in the research. The main advantage of PCA is the possibility of evaluating data variance and, through loadings, of understanding which kind of signal has been obtained (not only the peaks but also the noise). By using PCA, it is possible to choose the best pre-processing methods in order to make the data comparable between the two different instruments.

2. Research aim

The main aim of this work is to evaluate the potential of two X-ray fluorescence instruments, laboratory and portable, in order to propose operative procedures in the context of cultural heritage.

In order to evaluate the results from the two different instruments, well-known and characterized yellow pigments based on lead, tin and antimony were chosen. These pigments, as already mentioned, were prepared in our laboratory according to ancient recipes and also according to the stoichiometric ratio of the chemical elements in the final products. Following this strategy, an XRF based comparison, not affected by uncertain compositions often associated with commercial pigments, was carried out handling the resulting spectra by a chemometric approach (i.e. principal component and multivariate analysis) with the specific aim of verifying the spectral differences, and related informative content, between the different produced yellow pigments. XRF spectroscopy, as previously outlined, is a technique widely used in painting analysis due to its non-invasive and non-destructive characteristics. It has also been used for identifying and differentiating yellow pigments based on lead, tin and antimony, but some uncertainty remained due to the similar composition of these yellows and also due to the presence of other pigments often mixed with yellows, such as lead white or copper based compounds, which could alter element ratios and colour characteristics [44–46]. The possibility of differentiating yellow pigments, especially that based on lead and antimony, produced according to different recipes, is particularly relevant in artwork examination through the XRF technique. Indeed, this makes it possible to gather information on the period of production, the workshop and the geographical area [44,47–49].

3. Experimental

3.1. Investigated pigments

Eleven pigments samples were selected for the X-ray fluorescence spectroscopic investigation (Table 1). The chosen pigments were prepared according to both the stoichiometric ratios of the final compounds and the indications supplied by the recipes [36,38]. The quantities of reagents in the recipes are reported in Libras (ancient Roman measure equal to 327 g). Some pigments, one for each typology, were then selected for preparing paintings on commercial canvas and wood support. Both kinds of support were prepared by applying a traditional setting made of gypsum and glue. The commercial canvas may contain additives used to prepare the support, such as titanium white. The chosen pigments are: PSA2 (lead/tin yellow type I, prepared according to the Pb:Sn = 2:1 molar ratio), PSB3 (lead/tin yellow type II, prepared according to the stoichiometric ratio of Pb and Sn, starting from PSA2 with the addition of silica), APA3 (lead/antimony yellow, prepared according to the stoichiometric ratio of Pb and Sn) and APSA (lead/tin/antimony yellow, prepared according to the stoichiometric ratio of Pb, Sn and Sb). They were applied by linseed oil and rabbit skin glue binders.

3.2. Scanning electron microscopy-energy dispersive spectroscopy (SEM-EDS)

Yellow pigments were examined by SEM-EDS by using a JSM 5400 system with SIRIUS-SD 10128 LE electron probe micro analysis supplied by iXFR Systems. The crystal area is 10 mm^2 and the work distance 20 mm. The probe operated at 25 kV and 80 mA.

3.3. X-ray fluorescence spectroscopy set-up

X-ray fluorescence analysis was performed with the following instruments:

- Bruker Tornado M4 equipped with a Rh tube, operating at 50 kV, 500 μA, spot 25 μm obtained with polycapillary optics [50];
- Assing Surface Monitor II equipped with Au tube, operating at 50 kV, 300 μA, spot 2 mm.

For each sample powder, 20 points of measurements were executed at three different acquisitions times: 30 s, 60 s and 240 s. In

Table 1
Description of the samples used for XRF analysis.

Sample abbreviation	Production conditions	Pigment
PSA2	Pb_3O_4 (3.0 g), SnO_2 (1.0 g), Pb:Sn = 2:1 molar ratio, 800 °C in porcelain crucible	Lead/tin yellow type I (stoichiometric ratio of Pb and Sn)
CPbSnA1	Metallic Pb (9.8 g) and Sn (10.8 g), 800 °C for 5 hours in refractory crucible	Calcined lead and tin by Danzica manuscript recipe 13/c 3.v
CPbSnD	Metallic Pb (1.30 g) and Sn (0.32 g), 800 °C for 5 hours in refractory crucible	Calcined lead and tin by Cipriano Piccolpasso
PSB3	PSA2 (2.0 g), SiO_2 (0.2 g), 800 °C for 5 hours in porcelain crucible	Lead/tin yellow type II (stoichiometric ratio of Pb and Sn)
PSMSBZA	Calcined lead/tin (CPbSnD, 6.54 g), paternoster (6.54 g, recipe 272 of Bolognese Manuscript), Pb_3O_4 (8.18 g), SiO_2 (1.63 g), 800 °C on terracotta plate	*Zallolin de depentori*, recipe 273 of the Bolognese Manuscript
APA3	Pb_3O_4 (5.94 g), Sb_2O_3 (3.7 9g), 900 °C on terracotta plate covered by paper	Lead antimonate (Naples yellow). Stoichiometric ratio of Pb and Sb
PSAPPA1	Sb_2O_3 (1.30 g), Pb_3O_4 (1.90 g), $C_4H_5KO_6$ (lees, 0.30 g), 800 °C for 5 hours on terracotta plate	*Zallolin* by Piccolpasso and Passeri common recipe
PSAPZ1	Sb_2O_3 (3.27 g), Pb_3O_4 (4.91 g), $C_4H_5KO_6$ (2.76 g), NaCl (2.76 g), 800 °C for 5 hours on terracotta plate	*Zallolino A* by Piccolpasso
PSAPZB1	Sb_2O_3 (0.66g), Pb_3O_4 (0.98g), $C_4H_5KO_6$ (0.32g), NaCl (0.01g), 800 °C for 5 hours on terracotta plate	*Zallolino B* by Piccolpasso
APSA	PbO (1.78 g), SnO_2 (0.60 g), Sb_2O_3 (0.58 g), 925 °C for 5 hours on terracotta plate	Lead/tin/antimony yellow (stoichiometric ratio of Pb, Sn and Sb)
APSABR	Pb_2O_3 (3.27 g), SiO_2 (1.14 g), Sb_2O_3 (0.32 g), calcined lead/tin (CPbSnA1, 0.49 g), PbO (0.82 g)	Giallo in corpo by Danzica Manuscript 123 (c. 30r)

total, 1320 spectra were obtained, 660 for portable instrument and 660 for laboratory apparatus. The choice to perform the analysis on 20 points was due to the variability in composition of the pigments, especially of those prepared according to the recipes, as revealed by morphological and chemical analysis made by scanning electron microscopy coupled with energy dispersive spectroscopy. The paintings were analysed with the two instruments by acquiring 20 points for each pigment and binder selecting time 60 s, on the basis of the results obtained by the XRF analysis on powders.

Moreover, the laboratory instrument was also used to perform a mapping of the painting samples. The conditions for mapping are the following: width 672 pixel, height 426 pixel, pixel size 100 μm and pixel time 6.53 ms. The low acquisition time allows for creating a distribution "hypermap" of elements where each pixel is composed of XRF spectrum. This modality can be considered as complementary to point analysis and it allows the distribution of each investigated element to be gathered.

3.4. Data treatment and chemometric analysis

The spectral data analysis was carried out by standard chemometric methods. PLS_Toolbox (Version 7.8 Eigenvector Research, Inc.) running inside Matlab (Version 7.11.1, The Mathworks, Inc.) was used. In particular, principal component analysis (PCA) was applied. PCA is a powerful and versatile method capable of providing an overview of complex multivariate data and it is widely adopted to treat XRF data both from in situ analysis [51–54] and laboratory applications [55–57]. PCA can be used to reveal relations between variables and samples (i.e. clustering), detecting outliers, finding and quantifying patterns, generating new hypotheses as well as many other applications. It is used to decompose the processed spectral data into several principal components (PCs), linear combinations of the original spectral data, embedding the spectral variations of each collected spectral data set [58]. According to this approach, a reduced set of factors is produced. Such a set can be used for exploration, since it provides an accurate description of the entire dataset. The first few PCs, resulting from PCA, are generally used to analyse the common features among samples and their grouping: in fact, samples characterized by similar spectral signatures tend to aggregate in the score plot of the first two or three components [59]. Spectra could be thus characterized either by the intensity of peaks at characteristic X-ray line energies (KeV), or by their score on each PC in the PCs space. Samples exhibiting similar spectra are grouped in a region of the score plot in relation to the first two or three PCs, whereas samples with different spectral features will be clustered in other parts of this space. The advantage of using PCA concerns the possibility of exploring a large data set and so of comparing the results obtained by the two different instruments (portable and laboratory). The differences between instruments and data variability cannot be obtained with the average spectrum. Finally, loadings of each model show information about the characteristics of the spectra and their variability.

Pre-processing was adopted to emphasize the obtained results. Concerning the data gathered by p-XRF spectrometer with different acquisition times, pre-processing consisted of variable alignment, performed to reduce the shift effect of peak, normalize and mean center in order to center the data. Pre-processing for benchtop XRF data was normalized and mean centered.

Concerning the analysis of the painting samples, a baseline correction, to reduce the noise related to organic binders, followed by normalization and mean center pre-processing was applied. Finally, for the mapping of elements on the painting samples, smoothing was applied in order to reduce the effect of data noise. Moreover, normalize and mean center were used.

4. Results and discussion

4.1. SEM-EDS analysis on sample powders

The produced powders were characterized by SEM-EDS on different points layered on the stubs for SEM. The results of SEM-EDS analysis are summarized in Table 2. By considering the general results, it can be assessed that the pigments prepared according to the ancient recipes contain mixtures of compounds.

SEM-EDS analysis on sample CPbSnA1 (lead/tin yellow type I, prepared according to the Danzica manuscript) reveals the presence of an excess of tin. Generally tin oxide was detected by micro-Raman spectroscopy in almost all powders obtained following the indications of the recipes [36]. Only the calcined lead/tin pigment obtained by Piccolpasso recipe (sample CPbSnD) has homogeneous composition, in terms of chemical elements, and it is constituted by the compound Pb_2SnO_4 [36].

According to this result, lead and tin yellow type II was prepared by using the compound CPbSnD. The SEM-EDS analysis performed on the obtained sample (PSMSBZA) has homogeneous composition

Table 2
Results of SEM-EDS analysis in terms of molar proportion.

Sample abbreviation	SEM-EDS (molar proportion)	Notes
PSA2	Pb = 2; Sn = 1.1	Pb_2SnO_4 can be hypothesised
CPbSnA1	Pb = 1.2; Sn = 4.7	Evident excess of tin
CPbSnD	Pb = 2.6; Sn = 1.5 Pb = 3.1; Sn = 1.6	Mixture of compounds
PSB3	Pb = 2.3; Sn = 1.5; Si = 1.5	$PbSnO_3$ or $PbSn_{1-x}Si_xO_3$ can be hypothesised
PSMSBZA	Pb = 3.2; Sn = 1.5; Si = 1	$PbSnO_3$ or $PbSn_{1-x}Si_xO_3$ can be hypothesised
APA3	Pb = 2.2; Sb = 2.3 Pb = 1.4; Sb = 3.9	Mixture of compounds
PSAPPA1	Pb = 2.4; Sb = 2.4; K = 0.2 Pb = 2.3; Sb = 2.5; K = 0.2 Pb = 2.3; Sb = 3.1; K = 0.2	Mixture of compounds
PSAPZ1	Pb = 2.2; Sb = 3.2; Na = 0.5 Pb = 1.7; Sb = 4.0; Na = 0.08	Mixture of compounds
PSAPZB1	Pb = 2.0; Sb = 3.1; K = 0.1 Pb = 2.5; Sb = 2.6; K = 0.2 Pb = 1.8; Sb = 3; K = 0.1; Na = 0.1	Mixture of compounds
APSA	Pb = 2.7; Sb = 1.0; Sb = 1.0	$Pb_2SnSbO_{6.5}$ can be hypothesised
APSABR	Pb = 2.0; Sb = 0.5; Sn = 0.3	Evident excess of lead

in terms of chemical elements and so it can be associated to the formula $PbSn_{1-x}Si_xO_3$ [36].

A more complex situation can be found in the case of lead antimonate yellows. In all powders, different molar proportions were obtained in the points examined by SEM-EDS, suggesting the presence of various compounds as previously found and widely discussed in the literature [36–39,44,47,60–62]. Also sample APA3, prepared according to the stoichiometric ratio of Pb and Sb in the final compound ($Pb_2Sb_2O_7$), contains other compounds due to the different molar proportions, in respect to that expected, found in some examined points. In these points, the presence of rosiatite ($PbSb_2O_6$) was hypothesized in accordance with the excess of Sb compared to Pb [36,62].

In the samples prepared according to the recipes, potassium and sodium were also detected by SEM-EDS, due to the use of lees and/or NaCl as ingredients.

Lastly, SEM-EDS on lead/tin/antimony yellow prepared according to the stoichiometric ratio of the chemical elements, gives molar proportions compatible with the compound $Pb_2SnSbO_{6.5}$ [36,44,62]. On the other hand, the sample prepared according to the recipe 123 of Danzica manuscript (APSABR) exhibits molar proportion of the chemical elements characterised by excess of Pb in respect to Sn and Sb. This result seems to suggest the probable presence of other lead compounds in addition to the expected pigment ($Pb_2SnSbO_{6.5}$).

In conclusion, SEM-EDS analysis revealed that lead/tin yellows and lead/tin/antimony yellows with the expected formula seem to be produced if a stoichiometric ratio of the elements is used. Otherwise, mixtures of compounds were obtained. On the other hand, lead/antimony yellows always consist of mixtures, as previously observed by various authors [36–39,44,47,60–62]. On the base of this result, it was decided to perform the XRF analysis on several points (twenty) of the powder samples in order to account for this variability.

4.2. Analysis on sample powders and comparison between p-XRF and benchtop XRF

The results of our approach are now described in terms of acquisition times and the XRF equipment used. With regard to 30 s acquisition time, the PCA applied to the data obtained from the p-XRF shows good separation by using three principal components (Fig. 1A). The score plot highlights five different clouds corresponding to five different compositions of the examined powders. The combination of the first and second component allows for separating APSABR from CPSbA1, while the second component makes it possible to separate APSA from the lead-tin samples (CPSnD, PSA2, PSMBZA, PSB3) and from lead-antimony samples (APA3, PSAPZ1, PSAPPA1, PSAPZB1). The combination of the three components emphasizes the differences between sample APA3 and the other ones based on lead-antimony. Moreover, it allows for highlighting differences between samples PSA2 and CPSnD and the others containing lead and tin in their composition.

The first loading shows the variability of the peaks at 10.6 KeV and 12.7 KeV related respectively to Lα and Lβ of lead for the positive value (Fig. 1A). The variability of the peak at 3.5 KeV, 25.5 KeV, and 28.8 KeV are related respectively to Lα, Kα and Kβ of tin.

The second component is mainly influenced by tin (positive) and antimony (negative) peaks (Fig. 1A). The peaks at 3.9 KeV, 26.6 KeV and 30.0 KeV are related respectively to Lβ, Kα and Kβ of antimony. The variability in the loadings plots allows the separation of yellow samples on the base of peak ratios over 10 KeV. However, the model exhibits low sensitivity when separating samples containing light elements, such as silicon, sodium or potassium (PSB3, PSMSBZA, PSAPZB1), in this case, the clouds are superimposed. Sample CPbSnA1, prepared according to the recipe of Danzica manuscript (Table 1), is clearly different from the other ones, due to the presence of an excess of tin in the produced powder (Fig. 1A blue triangles), so it can be easily differentiated from the other pigments based on lead and tin. The third component is mainly influenced by lead and tin, on positive values, and by lead and antimony, on negative values, with a similar pattern observed for PC2 loading. The loadings of PC2 and PC3 show a shift effect for the peaks at 10.6 KeV and 12.7 KeV due to Lα and Lα of lead. P-XRF spectrometer working in the air condition is not capable of determining light elements. On the contrary, benchtop the XRF spectrometer, operating in a vacuum, is also able to analyse light elements. The loading plot highlights this difference, and it reveals better signals of the portable instrument for energy values over 10 KeV.

The PCA, applied to the data obtained by the laboratory instrument with 30 s acquisition time, shows a better separation of all different mixtures (Fig. 1B). The PCA score plot shows four main clouds, using the first two principal components: sample with excess tin (CPbSnA1), sample with lead-tin-antimony (APSABR), samples containing only lead and tin (APSABR, PSA2, CPbSnD, PSB3, PSMSBZA) and samples based on lead and antimony (PSAPZ1, PSAPPA1, PSAPZB1, APA3). The combination of the three principal components (total captured variance 98.11%) allows the separation of all samples according to the different ratio of the chemical elements (Fig. 1B). The loading of PC1 shows the variability at 3.3 KeV and 3.6 KeV due to Lα1 and Lβ1 of tin. The variability of the peak at 2.3 KeV, 10.3 KeV and 12.7 KeV are due respectively to Mα, Lα2 and Lβ of lead. The second component shows the variability of tin, for positive values, and antimony, for negative ones. The loadings of PC2 show the variability at 3.3 KeV related of Lα2 of antimony and 3.8 KeV due to Lβ of tin. The third component shows the variability of lead concentrations in all samples; PC3 loading is characterised by the variability of peaks at 2.3 KeV, 10.3 KeV and 12.7 KeV related respectively to Mα, Lα2 and Lβ of lead. By examining the variance in the loadings, it is possible to derive that the distribution of sample CPbSnA1 in the score plot is influenced by the high content of tin, the distribution of sample PSAPZ1 is influenced by the presence of antimony, while the distribution of sample PSA2 is mainly influenced by the intensity of lead peak. The combination of the three principal components also allows samples with different concentration ratios, such as APSABR to be identified. This sample, in fact, contains an excess of lead and may be clearly separated from the other samples based on lead-tin-antimony. The results

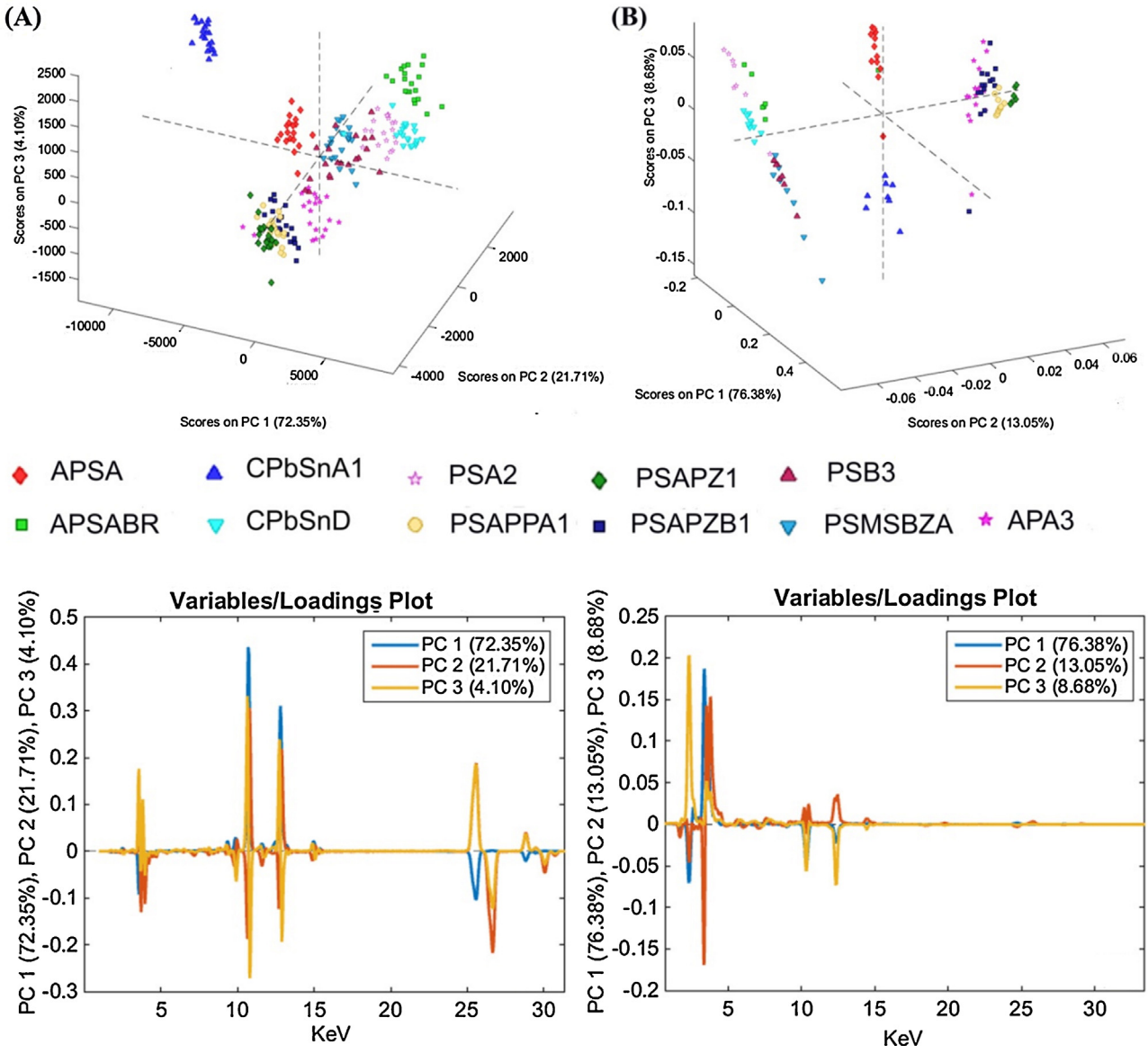

Fig. 1. Score plot of PCA and loadings (PC1, PC2 and PC3) applied to the detected XRF peaks for acquisition time 30 s, portable (A) and laboratory (B) instruments.

of the PCA model agree with the compositional data obtained by SEM-EDS.

Comparing the results obtained with the two different instruments, it is possible to observe that a good separation of yellow pigments based on antimony and lead (APA3, PSAPZB1, PSAPPA1, PSAPZ1) can be reached with the laboratory instrument and not with the portable apparatus (Fig. 1). For the other mixtures, the results gathered with the two spectrometers are similar.

The results obtained with the acquisition time set to 60 s show variability and characteristics similar to those gathered for 30 s, in particular concerning the portable instrument (Fig. 2). On the other hand, the laboratory system shows better resolution at acquisition time 60 s compared to 30 s, with an overlay of spectra for the pigments of the same class (Fig. 2A). The second component has greater variability for high values of tin (see the outlier CPbSnA1, Fig. 2B). The third component allows for the evaluation of the variance of lead for each spectrum. By observing the score plot for the portable instrument, it is possible to see good separation between pigments containing lead and antimony (PSAPPA1, PSAPZ1, PSAPZB1, and APA3) and between pigments based only on tin and lead (especially CPbSnD, PSA2, PBMSBZA, PSB3). The distribution observed for the data collected by portable XRF are confirmed with the laboratory instrument highlighting the same grouping (Fig. 2A and B).

Lastly, the loadings plots of PCA data are reported in Fig. 3 for acquisition time 240 s. Regarding the laboratory instrument, a significant reduction in variability of the 10.6 KeV and 12.7 KeV peaks, due to Lα and Lβ of lead, can be observed, if compared to the same data at 30 s and 60 s acquisition times. For this reason, the information regarding lead can be gathered only by the negative area of PC1 and PC3.

By observing the score plots (Fig. 3A), it can be derived that the 240 s distribution exhibits no significant changes in terms of separation of pigment groups, compared to the 60 s one. The laboratory instrument (Fig. 3B) allows a clear separation of the lead antimonate yellows and lead/tin yellows.

As previously underlined, the benchtop XRF, operating under vacuum, allows better detection of elements under 10 KeV, so with long acquisition times (60 s and 240 s), high quality of each spectrum is observed. PCA applied on data from benchtop instruments makes it possible to obtain good separation of all examined powders whereas the differences in signals at 60 s and 240 s gathered from p-XRF are not so evident.

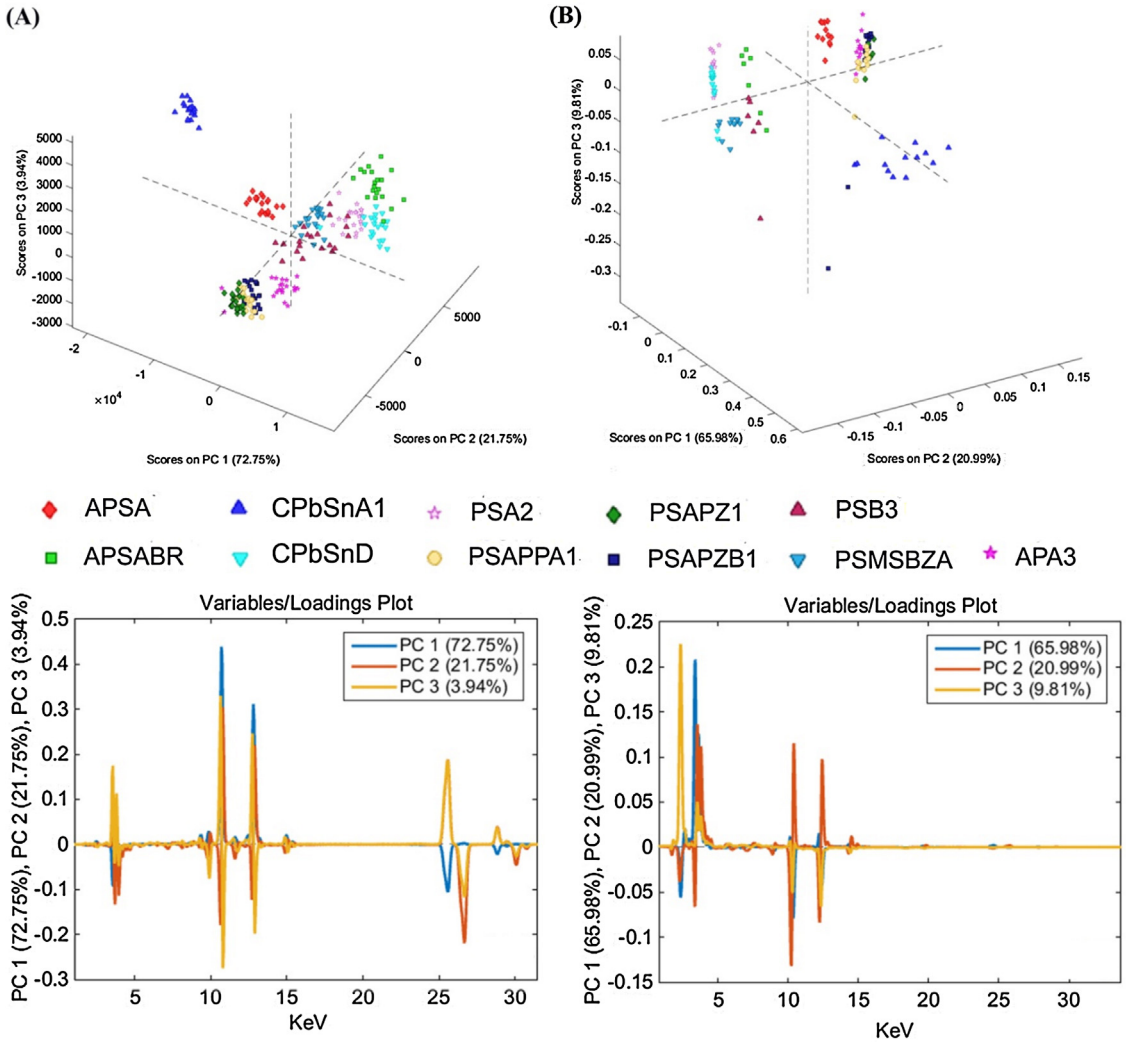

Fig. 2. Score plots of PCA and loadings (PC1, PC2 and PC3) applied to the detected XRF peaks for acquisition time 60 s, portable (A) and laboratory (B) instruments.

4.3. Simulation of paint layers

4.3.1. Analysis on paint layers and comparison between p-XRF and benchtop XRF

When investigating real paintings, several factors should be evaluated, such as pigment layer thickness, matrix effects, presence of different pigments, presence of setting layers and support. All these factors make the quantitative characterization of a specific pigment in real artworks difficult. However, if on the one hand, it is very difficult to gather quantitative measurements, on the other, it is possible to obtain qualitative information on the different element ratios in an investigated pigment. For this reason, in order to evaluate only the variance that can be attributed to the pigment and not that due to the elements in the setting layers or in the support, the energies from 3.5 to 5 KeV were excluded.

Starting from the results of XRF analysis on powders, some paintings, prepared with chosen yellow pigments and binders applied on different supports were examined. The selected acquisition time for the painting samples, considering the results obtained for the pigment powders, was 60 s (Fig. 4). PCA score plot of p-XRF measurements shows a good separation between samples APSA, APA2 and PSA2/PSB3 without a distinction between PSA2 and PSB3 (Fig. 4A). On the contrary, the analysis performed by benchtop XRF gives four separated clouds corresponding to the four different yellows (Fig. 4B). The analysis of loadings from p-XRF and benchtop XRF on paintings shows a variance of the data similar to that observed for powder pigments in the same spectrum regions: this result was made possible by excluding peaks associated with the elements of the support (calcium and titanium). The high sensitivity of benchtop XRF detector, combined with the measure under vacuum conditions, shows better silicon peak resolution and allows the PCA model to separate PSB3 from PSA2 (Fig. 4B).

4.3.2. Mapping on painting samples by benchtop XRF

Taking the results obtained by a multipoint approach as a starting point, the paintings were acquired in mapping modality by micro-XRF. The data were then elaborated by PCA. The study of mapping modality, possible in this case only with the benchtop instrument, aimed to investigate the real situation of a painting layer whose thickness and pigment concentration are not known. In the mapping approach, all spectra are analysed to evaluate the variability of the data for each paint layer. The composition of the setting layer (containing calcium, sulphur, or titanium) has a low variability in comparison to that of the elements in the investigated yellow pigments. Therefore, it can be affirmed that the variability in the PCA model depends mainly on the thickness and composition of yellow in the layers. The mapping mode is complementary to point analysis and allows the identification of the distribution of chemical elements in the pictorial layer and the evaluation of the differences due to the thickness of the pictorial layer and due to the

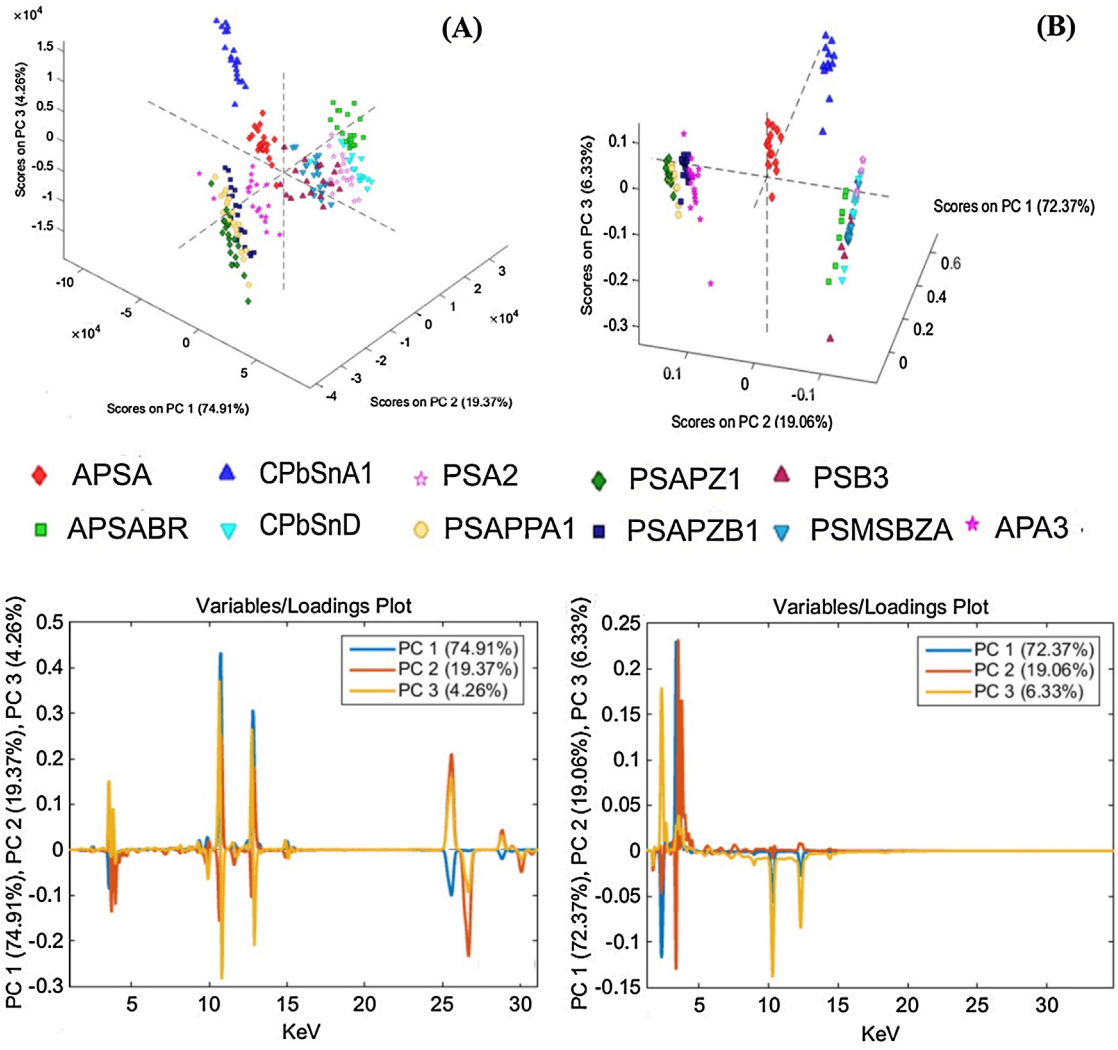

Fig. 3. Score plots of PCA and loadings (PC1, PC2 and PC3) applied to the detected XRF peaks for acquisition time 240 s, portable (A) and laboratory (B) instruments.

concentration of pigments inside medium. Greater thickness of the painted layer cause a reduction of the peak intensity attributable to the setting layer; lower concentration of the pigment in the medium decreases the intensity of the peaks associated with the pigment itself, so in order to evaluate the combination of these factors, in addition to the variability of each pigment, an exploratory approach such as PCA can be useful.

Concerning the oil and glue paintings on canvas, titanium is contained in the white layer of the commercial canvas (Fig. 5). This element exhibits great variability, so that, in order to better investigate the variability of only the yellow paintings, it was necessary to select PC1, showing mainly the variability of Ti as positive values and lead as negative values, and PC3 highlighting the combined variability of lead, tin, antimony and silicon. Indeed, PC2 has a high influence of titanium. For PSB3, the scores plot shows a distribution mainly influenced by the positive values of the first component. The separation of the other yellow paintings occurs along the third component. Sample APSA is positioned in the centre of the score plot; PSA2 and APA3 are influenced by the positive and negative values of PC3, respectively.

The mapping results of the glue and oil paintings on wood are reported in Fig. 6.

The first loading shows the variability of tin and antimony as positive values, and that of lead as negative. The second loading highlights the combined variability of lead, tin and antimony and to a lesser extent those of calcium and silicon. For PSB3, the scores plot shows a distribution similar to that observed in the previous case, mainly influenced by the positive values of the first component. The other painting samples are separated along the third component. Sample APSA appears in a central position of the scores plot, as observed for painting on canvas. At last, PSA2 and APA3 paintings are influenced respectively by the positive and negative values of the third component.

5. Conclusions

In this study, two XRF spectrometers were used to investigate the possibility of discriminating a group of yellow pigments based on lead, tin and antimony prepared in our laboratory according to both stoichiometric ratios of the elements and to ancient recipes. In particular, a portable instrument supplied by Assing S.p.A. (i.e. Surface Monitor II portable unit) and a laboratory apparatus by Bruker (i.e. Tornado M4 laboratory unit) were tested in order to make a comparison between the spectrometer performances and also to find the most appropriate acquisition time. This last topic is of particular relevance in the case of in situ analysis that generally requires short times of acquisition. So, the possibility to obtain the "right" acquisition time is fundamental in cultural heritage analysis using the XRF technique.

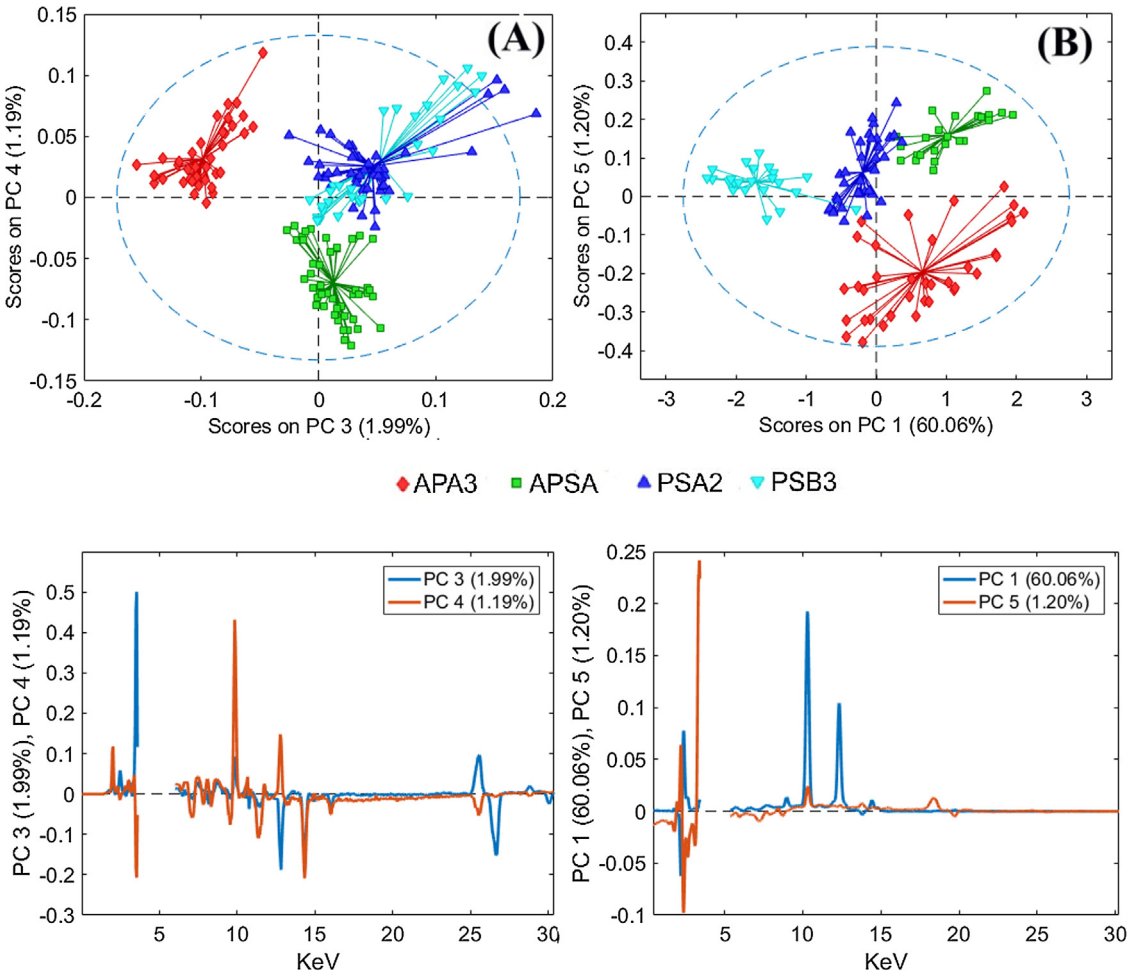

Fig. 4. Scores plots of PCA and loadings by portable (A) and laboratory (B) instruments obtained for the three different binders (linseed oil, glue and egg) and supports (canvas, wood, mortar).

The experimental data, collected both by portable and laboratory spectrometers, were elaborated by PCA and multivariate tools to verify the spectral differences and the related informative content among the different produced yellow pigments. The use of loadings plots for PCs representation, as a function of energies expressed in KeV, was useful to highlight the variability of the elements and to stress the relevance of each XRF peak. The portable instrument showed a better spectral resolution for energy values over 10 KeV whereas the laboratory micro-spectrometer has a better resolution for energy values less than 10 KeV. The comparison between the data obtained at the three acquisition times, demonstrated that the results gathered with 60 s and 240 s are not significantly different, suggesting 60 s as the best acquisition time for XRF measurements.

Yellow pigments based on lead and antimony, but produced according to different recipes, can be well differentiated through XRF analysis applied in this work with the described approach. This result is interesting from a practical point of view because it demonstrates the possibility of gathering information, through non-invasive analysis, on the period of production, the workshop and the geographical area of antimonate yellows.

The experimental approach used in the present work, also demonstrated the possibility of differentiating pigments, based on tin and lead, produced according to different recipes (see for example lead/tin yellow produced according to the Danzica manuscript) and procedures: type I and type II are well separated in the score plots of PCA especially at 60 s and 240 s times of acquisition, both for portable and laboratory apparatus. A good separation was also obtained for the two yellows based on lead, tin and antimony (APSA and APSABR).

The analytical approach used for pigment powders was tested on paintings applied by different binders on two kinds of support. The analysis on the paintings was clearly more complex to perform due to the presence of other elements (Ca, S and Ti) not contained in the yellow pigments. In this case, further elaboration and data treatment were necessary to eliminate the contributions of these elements. The scores plot, obtained by portable and laboratory instruments applied on paintings, showed the possibility for good separation of the lead antimonate yellow (APA3) and lead/tin/antimony yellow (APSA), whereas lead/tin yellows type I and type II are not well differentiated, especially with the portable instrument.

Finally, a mapping approach was utilized to investigate the possibility of discriminating the paintings by applying the specific tool of the Bruker micro-spectrometer.

Despite the complexity of the system, due to the presence of peaks attributable to the support and to the setting layer, it was possible to identify, through PCA, spectral differences between the examined paintings. This result is particularly relevant, in our opinion, because it allows for the evaluation of the variability and the distribution of each examined pictorial layer. Mapping demonstrated the possibility to clearly discriminate lead/antimony and lead/tin/antimony yellows in the score plot of the PCA model.

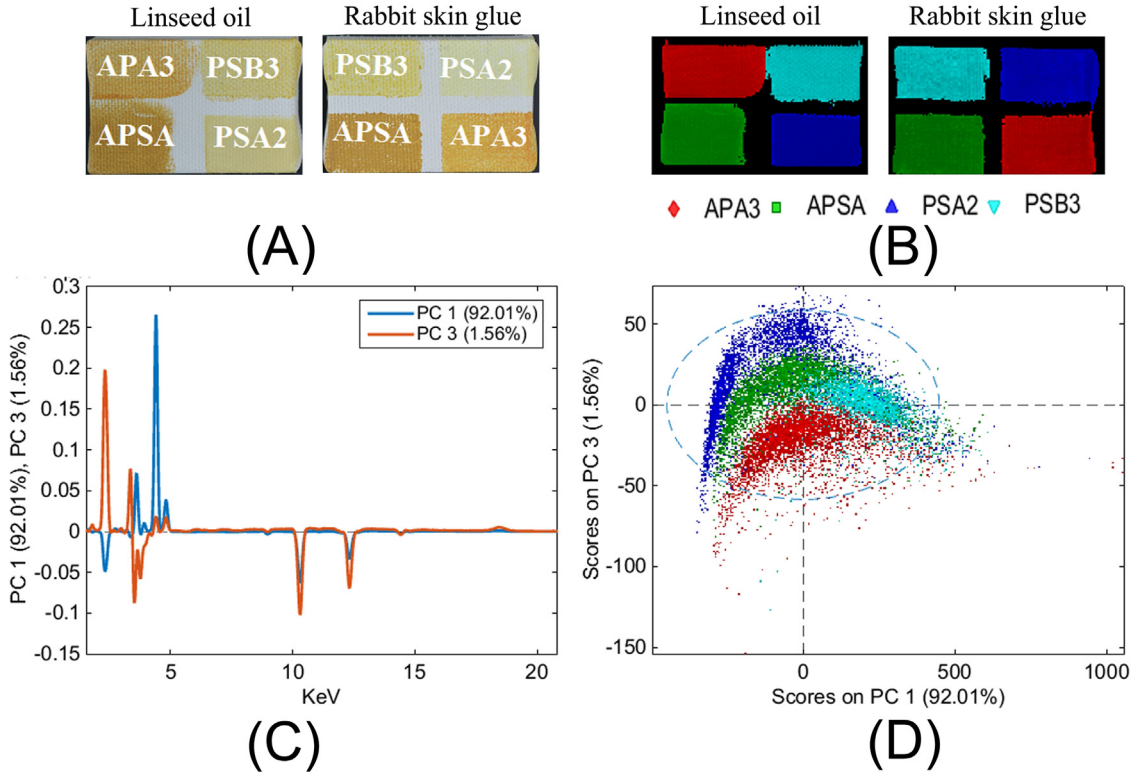

Fig. 5. Results of XRF mapping on pigments applied on canvas; RGB image of sample (A), cube of data with class set (B), loading of PCA model (C), score plot of PCA model (D).

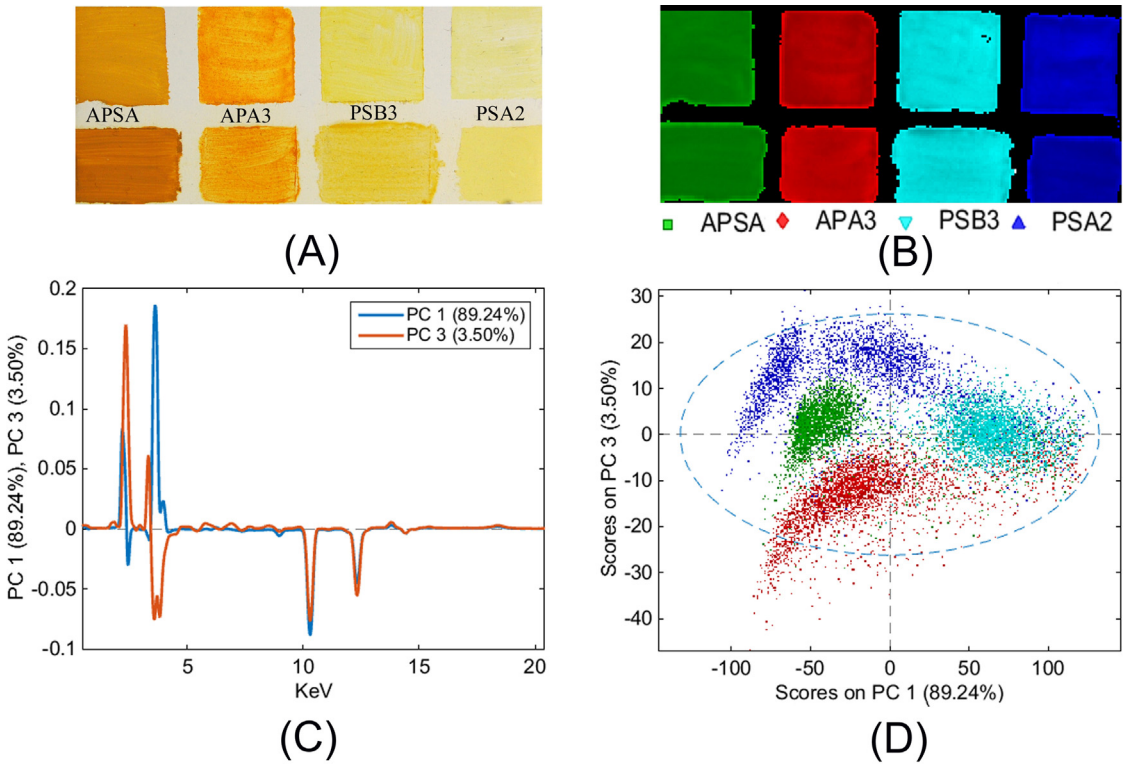

Fig. 6. Results of XRF mapping on pigments applied on wood; RGB image of sample (A), cube of data with class set (B), loading of PCA model (C), score plot of PCA model (D).

Lead/tin yellows are more difficult to differentiate. A large variability of data, related to the thickness of the painting layers and to the concentration of the pigment in the different binders, has also been observed.

The mapping approach can be considered as a preliminary procedure requiring further tests to confirm its validity, also with reference to different pigments. Nevertheless, the preliminary results presented in this paper encourage the continuation of this

research in order to verify the possibility of developing and fully utilizing automatic classification models for the identification of pigments.

Acknowledgements

The authors would like to thank Assing S.p.A. for having supplied the Surface Monitor II for testing in pigment analysis, in particular Dr. Luigi Iozzoli, the product manager.

References

[1] R. Jenkins, X-ray fluorescence spectrometry, Second Edition, Wiley, 1999.
[2] M. Mantler, M. Schreiner, X-ray fluorescence spectrometry in art and archaeology, X-Ray Spectrom. 29 (2000) 3–17.
[3] P. Moioli, C. Seccaroni, Analysis of art objects using a portable X-ray fluorescence spectrometer, X-Ray Spectrom. 29 (2000) 48–52.
[4] C. Seccaroni, P. Moioli, Fluorescenza X. Prontuario per l'analisi XRF portatile applicata a superfici policrome, Nardini Editore, Firenze, 2002.
[5] R. Cesareo, S. Ridolfi, M. Marabelli, A. Castellano, G. Buccolieri, M. Donativi, G.E. Gigante, A. Brunetti, M.A. Rosales Medina, Portable systems for energy-dispersive X-ray fluorescence analysis of works of art, in: P.J. Philip, M. West (Eds.), Portable X-ray fluorescence spectrometry: capabilities for in situ analysis, RSC Publishing, Cambridge, 2008, pp. 206–246.
[6] R. Cesareo, G.E. Gigante, A. Castellano, S. Ridolfi, Portable and handheld systems for energy-dispersive X-ray fluorescence analysis, in: Encyclopedia of Analytical Chemistry, 2009.
[7] K. Janssens, G. Van der Snickt, F. Vanmeert, S. Legrand, G. Nuyts, M. Alfeld, L. Monico, W. Anaf, W. De Nolf, M. Vermeulen, J. Verbeeck, K. De Wael, Non-invasive and non-destructive examination of artistic pigments paints, and paintings by means of X-ray methods, in: R. Mazzeo (Ed.), Analytical Chemistry for Cultural Heritage, Springer, Cham, Switzerland, 2016, p. 77-128.
[8] A.N. Shugar, J.L. Mass (Eds.), Handheld XRF for Art and Archaeology, University Press, Leuven, 2012.
[9] A.M.W. Hunt, R.J. Speakman, Portable XRF analysis of archaeological sediments and ceramics, J. Archaeol. Sci. 53 (2015) 626–638.
[10] F.-P. Hocquet, H. Calvo del Castillo, A. Cervera Xicotencatl, C. Bourgeois, C. Oger, A. Marchal, M. Clar, S. Rakkaa, E. Micha, D. Strivay, Elemental 2D imaging of paintings with a mobile EDXRF system, Anal. Bioanal. Chem. 399 (2011) 3109–3116.
[11] K. Trentelman, M. Bouchard, M. Ganio, C. Namowicz, C. Schmidt Patterson, M. Walton, The examination of works of art using in situ XRF line and area scans, X-Ray Spectrom. 39 (3) (2010) 159–166.
[12] G. Sciutto, P. Oliveri, S. Prati, M. Quaranta, S. Bersania, R. Mazzeo, An advanced multivariate approach for processing X-ray fluorescence spectral and hyperspectral data from non-invasive in situ analyses on painted surfaces, Anal. Chem. Acta 752 (2012) 30–38.
[13] G.E. Gigante, S. Ridolfi, D. Ferro, Diagnostic investigations and statistical validation of EDXRF mapping of the burial monument of Pope Sixtus IV by Antonio Pollaiolo (1493) in the Vatican, J. Cult. Herit. 13 (3) (2012) 345–351.
[14] E. Frahm, R.C. Doonan, The technological versus methodological revolution of portable XRF in archaeology, J Archaeol. Sci. 40 (2) (2013) 1425–1434.
[15] M.S. Shackley, Is there reliability and validity in portable X-ray fluorescence spectrometry (PXRF), SAA Archaeol. Rec. 10 (5) (2010) 17–20.
[16] E.T. Hall, X-ray fluorescent analysis applied to archaeology, Archaeometry 3 (1) (1960) 29–35.
[17] E.T. Hall, M.S. Banks, J.M. Stern, Uses of X-ray fluorescent analysis in archaeology, Archaeometry 7 (1) (1964) 84–89.
[18] T.C. Yao, F.H. Stross, The use of analysis by X-ray fluorescence in the study of coins, Am. J. Archaeol. 69 (2) (1965) 154–156.
[19] R.N. Jack, R.F. Heizer, "Finger-Printing" of some Mesoamerican obsidian artifacts Contributions of the University of California Archaeological Research Facility, 5, 1968, pp. 81–100.
[20] C. Jones, Don't mention Stonehenge!, Significance 5 (1) (2008) 46–48.
[21] S.C. Phillips, R.J. Speakman, Initial source evaluation of archaeological obsidian from the Kuril Islands of the Russian Far East using portable XRF, J. Archaeol. Sci. 36 (6) (2009) 1256–1263.
[22] G. Evans, R.F. Pettifer, CHOOCH: a program for deriving anomalous-scattering factors from X-ray fluorescence spectra, J. Appl. Crystallogr. 34 (1) (2001) 82–86.
[23] P.J. Potts, M. West (Eds.), Portable X-ray fluorescence spectrometry: capabilities for in situ analysis, Royal Society of Chemistry, 2008.
[24] S.J. Choi, C.H. Kim, S.G. Lee, Comparison of the heavy metal analysis in soil samples by bench-top ED-XRF and field-portable XRF, Anal. Sci. Technol. 22 (4) (2009) 293–301.
[25] M.B.B. Guerra, E. de Almeida, G.G. Carvalho, P.F. Souza, L.C. Nunes, D.S. Júnior, F.J. Krug, Comparison of analytical performance of benchtop and handheld energy dispersive X-ray fluorescence systems for the direct analysis of plant materials, J. Anal. Atom. Spectrom. 29 (9) (2014) 1667–1674.
[26] E. Marguí, M. Hidalgo, I. Queralt, K. Van Meel, C. Fontas, Analytical capabilities of laboratory, benchtop and handheld X-ray fluorescence systems for detection of metals in aqueous samples pre-concentrated with solid-phase extraction disks, Spectrochim. Acta B 67 (2012) 17–23.
[27] A.L.M. Silva, S. Cirino, M.L. Carvalho, M. Manso, S. Pessanha, C.D. Azevedo, J.F.C.A. Veloso, Elemental mapping in a contemporary miniature by full-field X-ray fluorescence imaging with gaseous detector vs. scanning X-ray fluorescence imaging with polycapillary optics, Spectrochim. Acta B 129 (2017) 1–7.
[28] T. Shiraiwa, N. Fujino, Theoretical calculation of fluorescent X-ray intensities in fluorescent X-ray spectrochemical analysis, Jpn. J. Appl. Phys. 5 (10) (1966) 886.
[29] Y. Hiraoka, A possible approach to soil discrimination using X-ray fluorescence analysis, J. Forensic Sci. 39 (6) (1994) 1381–1392.
[30] F. Colao, R. Fantoni, P. Ortiz, M.A. Vazquez, J.M. Martin, R. Ortiz, N. Idris, Quarry identification of historical building materials by means of laser induced breakdown spectroscopy X-ray fluorescence and chemometric analysis, Spectrochim. Acta B 65 (8) (2010) 688–694.
[31] F. Cariati, P. Fermo, S. Gilardoni, A. Galli, M. Milazzo, A new approach for archaeological ceramics analysis using total reflection X-ray fluorescence spectrometry, Spectrochim. Acta B 58 (2) (2003) 177–184.
[32] B. Vekemans, L. Vincze, F.E. Brenker, F. Adams, Processing of three-dimensional microscopic X-ray fluorescence data, J. Anal. Atom. Spectrom. 19 (10) (2004) 1302–1308.
[33] G.G. Bortoleto, E.A. De Nadai Fernandes, F.S. Tagliaferro, A.A. Ferrari, M.I. Bueno, Potential of X-ray spectrometry and chemometrics to discriminate organic from conventional grown agricultural products, in: 16th IFOAM Organic World Congress, Modena, Italy, 2008, available at http://orgprints.org/12348/.
[34] A.R. Kuzel, A.M. Christensen, S.M. Marvin, Calcium and phosphorus detection using Benchtop versus handheld X-ray fluorescence spectrometers, J. Forensic Sci. 61 (S1) (2016) S190–S192.
[35] P. Lemberge, P.J. Van Espen, B.A.R. Vrebos, Analysis of cement using low-resolution energy-dispersive X-ray fluorescence and partial least-squares regression, X-Ray Spectrom. 29 (4) (2000) 297–304.
[36] G. Agresti, P. Baraldi, C. Pelosi, U. Santamaria, Yellow pigments based on lead, tin and antimony: ancient recipes, synthesis, characterization and hue choice in artworks, Color Res. Appl. 41 (3) (2016) 226–231.
[37] C. Pelosi, U. Santamaria, G. Agresti, E. Mattei, A. De Santis, Production and characterisation of lead, tin and antimony based yellow pigments, in: J.H. Townsend, L. Toniolo, F. Cappitelli (Eds.), Conservation Science 2007, Archetype Publication, London, 2008, pp. 187–188.
[38] C. Pelosi, G. Agresti, U. Santamaria, E. Mattei, Artificial yellow pigments: production and characterization through spectroscopic method of analysis, e-Preserv. Sci. 7 (2010) 108–115.
[39] U. Santamaria, G. Agresti, C. Pelosi, Memory and matter of cultural heritage: lead, tin and antimony based yellow pigments Fatto díarchimia, in: M. del Egido, S. Kroustallis (Eds.), Los pigmentos artificiales en las técnicas pictóricas, Secretaría General Técnica Subdirección General de Publicaciones, Información y Documentación, Madrid, 2012, pp. 147–158.
[40] L. Chiarantini, F. Gallo, V. Rimondi, M. Benvenuti, P. Costagliola, A. Dini, Early Renaissance production recipes for Naples yellow pigment: a mineralogical and lead isotope study of Italian majolica from Montelupo (Florence), Archaeometry 57 (5) (2015) 879–896.
[41] K.F. Gebremariam, L. Kvittingen, F.-G. Banica, Application of a portable XRF analyzer to investigate the medieval wall paintings of Yemrehanna Krestos Church, Ethiopia, X-Ray Spectrom. 42 (2013) 462–469.
[42] I. Toulos, C. Papachristodoulou, K. Stamoulis, K. Ioannides, S. Pavlides, R. Caputo, A. Chatzipetros, I. Koukouvelas, E. Kremastas, The principal component analysis of X-ray fluorescence spectrometry data as a tool for paleoseismic, in: EGU General Assembly, Vienna Austria, id. EGU2013-6002, 2013.
[43] G. Visco, S.H. Plattner, G. Guida, S. Ridolfi, G.E. Gigante, Rings or daggers, axes or fibulae have a different composition? A multivariate study on Central Italy bronzes from Eneolithic to Early Iron age, Chem. Central J. 9 (2015) 15.
[44] D. Hradil, T. Grygar, J. Hradilová, P. Bezdička, V. Grűnwaldová, I. Fogaš, C. Miliani, Microanalytical identification of Pb-Sb-Sn yellow pigment in historical European paintings and its differentiation from lead tin and Naples yellows, J. Cult. Herit. 8 (4) (2007) 377–386.
[45] C. Pelosi, G. Agresti, D. Coralli, U. Santamaria, Applicazione della spettrocolorimetria e della spettroscopia di fluorescenza dei raggi X per la caratterizzazione di pigmenti in miscela, in: M. Rossi, A. Siniscalco (Eds.), Colore e Colorimetria contributi multidisciplinari, IX A, Maggioli Editore, Santarcangelo di Romagna (RN), 2013, p. 334-340.
[46] I. Borgia, B.G. Brunetti, C. Miliani, C. Ricci, C. Seccaroni, A. Sgamellotti, The combined use of lead/tin yellow type I and II on a canvas painting by Pietro Perugino, J. Cult. Herit. 8 (2007) 65–68.
[47] J. Dik, E. Hermens, R. Peschar, H. Schenk, Early production recipes for lead antimonite yellow in Italian Art, Archaeometry 47 (2005) 593–607.
[48] M. Maggetti, C. Neururer, J. Rosen, Antimonate opaque glaze colours from the Faience manufacture of le Bois d'Épense (19th century, northeastern France), Archaeometry 51 (5) (2009) 791–807.
[49] A. Bezur, F. Casadio, Studies in archaeological sciences, in: N. Aaron, Shugar, L. Jennifer, Mass (Eds.), Handheld XRF for Art and Archaeology, Leuven University Press, 2012, pp. 249–311.
[50] G. Bonifazi, G. Capobianco, S.S. Serranti, Hyperspectral imaging applied to the identification and classification of asbestos fibers (2015 November), in: SENSORS, IEEE, 2015, pp. 1–4.

[51] F. Rosi, A. Burnstock, K.J. Van den Berg, C. Miliani, B.G. Brunetti, A. Sgamellotti, A non-invasive XRF study supported by multivariate statistical analysis and reflectance FTIR to assess the composition of modern painting materials, Spectrochim. Acta A 71 (2009) 1655–1662.
[52] M. Sawczak, A. Kamińska, G. Rabczuk, M. Ferretti, R. Jendrzejewski, G. Śliwińskia, Complementary use of the Raman and XRF techniques for non-destructive analysis of historical paint layers, Appl. Surf. Sci. 255 (2009) 5542–5545.
[53] F. Rosi, C. Miliani, C. Clementi, K. Kahrim, F. Presciutti, M. Vagnini, V. Manuali, A. Daveri, L. Cartechini, B.G. Brunetti, A. Sgamellotti, An integrated spectroscopic approach for the non-invasive study of modern art materials and techniques, Appl. Phys. A 100 (3) (2010) 613–624.
[54] A. Pitarch, A. Ramón, A. Álvarez-Pérez, K. Castro, J.M. Madariaga, I. Queralt, Multispectroscopic characterization of oil on copper painting, Spectrosc. Lett. 47 (1) (2014) 38–51.
[55] F. Manhas, V. Pereira, M. Izabel, M. Silveira Bueno, Evaluation of varnish and paint films using digital image processing, energy dispersive X-ray fluorescence spectrometry, and chemometric tools, J. Coat. Technol. Res. 6 (4) (2009) 445–455.
[56] M.F. Alberghina, R. Barraco, M. Brai, T. Schillaci, L. Tranchina, Integrated analytical methodologies for the study of corrosion processes in archaeological bronzes, Spectrochim. Acta B 66 (2011) 129–137.
[57] R.J. Speakman, N.C. Little, D. Creel, M.R. Miller, J.G. Iñañez, Sourcing ceramics with portable XRF spectrometers? A comparison with INAA using Mimbres Pottery from the American Southwest, J. Archaeol. Sci. 38 (2011) 3483–3496.
[58] R. Bro, A.K. Smilde, Principal component analysis, Anal. Methods 6 (9) (2014) 2812–2831.
[59] G. Agresti, G. Bonifazi, L. Calienno, G. Capobianco, A. Lo Monaco, C. Pelosi, R. Picchio, S. Serranti, Surface investigation of photo-degraded wood by colour monitoring, infrared spectroscopy, and hyperspectral imaging, J. Spectr. 1 (1) (2013) (art. No. 380536).
[60] K. Sakellariou, C. Miliani, A. Morresi, M. Ombrelli, Spectroscopic investigation of yellow majolica glazes, J. Raman Spectr. 35 (2004) 61–67.
[61] C. Sandalinas, S. Ruiz-Moreno, Lead-tin-antimony yellow: historical manufacture, molecular characterization and identification in seventeenth-century Italian paintings, Stud. Conserv. 49 (1) (2004) 41–52.
[62] L.D. Kock, D. De Waal, Raman analysis of ancient pigments on a tile from the Citadel of Algiers, Spectrochim. Acta A 71 (2008) 1348–1354.